Molecular Pharmacology Fast Forward. Published on August 28, 2019 as DOI: 10.1124/mol.119.116129
This article has not been copyedited and formatted. The final version may differ from this version.

Title Page

Isoliquiritigenin, an orally available natural FLT3 inhibitor from licorice, exhibits selective anti-AML efficacy in vitro and in vivo

Zhi-Xing Cao[1,+], Yi Wen[2,3+], Jun-Lin He[1,+], Shen-Zhen Huang[4], Fei Gao[2,3], Chuan-Jie Guo[1], Qing-Qing Liu[2,3], Shu-Wen Zheng[1], Dao-Yin Gong[1], Yu-Zhi Li[1], Ruo-Qi Zhang[1], Jian-Ping Chen[1,2,3*] and Cheng Peng[1*]

* Corresponding authors

1. Pharmacy College, Chengdu University of Traditional Chinese Medicine; The Ministry of Education Key Laboratory of Standardization of Chinese Herbal Medicine; Key Laboratory of Systematic Research, Development and Utilization of Chinese Medicine Resources in Sichuan Province-Key Laboratory Breeding Base of Co-founded by Sichuan Province and MOST.

2. School of Chinese medicine, the University of Hong Kong

3. Shenzhen institute of research and innovation, University of Hong Kong

4. State Key Laboratory of Biotherapy and Cancer Center, West China Hospital, Sichuan University

[+] These authors contributed equally to this work.

Molecular Pharmacology Fast Forward. Published on August 28, 2019 as DOI: 10.1124/mol.119.116129
This article has not been copyedited and formatted. The final version may differ from this version.

Running Title Page

Running Title: Isoliquiritigenin inhibit AML cells via targeting FLT3

*Correspondence authors：

Jian-Ping Chen, Prof.; abchen@hku.hk

School of Chinese medicine, the University of Hong Kong

Cheng Peng, Prof.; pengchengchengdu@126.com; Tel: 86-28-61800234

Pharmacy College, Chengdu University of Traditional Chinese Medicine

Number of text pages: 39

Number of Tables: 2

Number of Figures: 5

Number of References: 52

Number of words in Abstract: 211 (must not exceed 250)

Number of words in Introduction: 660 (must not exceed 750)

Number of words in Discussion: 874 (must not exceed 1500)

List of abbreviations:

ISL – isoliquiritigenin;

AML – acute myeloid leukemia

FLT3 – fms-like tyrosine kinase-3

ITD – internal tandem duplications

TKD – tyrosine kinase domain

Molecular Pharmacology Fast Forward. Published on August 28, 2019 as DOI: 10.1124/mol.119.116129
This article has not been copyedited and formatted. The final version may differ from this version.

STAT5 – signal transducer and activator of transcription 5

MTT – 3-(4,5-dimethylthiazol-2-yl)-2,5-diphenyltetrazolium

DS – discovery studio

HTRF – homogeneous time -resolved fluorescence

TUNEL – terminal deoxynucleotidyl transferase-mediated dUTP-biotin nick end labeling

BM – bone marrow

PI – propidium iodide

Molecular Pharmacology Fast Forward. Published on August 28, 2019 as DOI: 10.1124/mol.119.116129
This article has not been copyedited and formatted. The final version may differ from this version.

ABSTRACT

Licorice is a medicinal herb widely used to treat inflammation-related diseases in China. Isoliquiritigenin (ISL) is an important constituent of Licorice and possesses multiple bioactivities. In this study, we examined the selective anti-AML (Acute myeloid leukemia) property of ISL via targeting FLT3, a certified valid target for treating AML. *In vitro*, ISL potently inhibited FLT3 kinase with an IC_{50} value of 115.1 ± 4.2 nM, selectively inhibited the proliferation of FLT3-ITD or FLT3-ITD/F691L mutant AML cells. Moreover, it showed very weak activity towards other tested cell lines or kinases. Western blot immunoassay revealed that ISL significantly inhibited the activation of FLT3/Erk1/2/STAT5 signal in AML cells. Meanwhile, Molecular docking study indicated that ISL could stably form aromatic interactions and hydrogen bonds within the kinase domain of FLT3. *In vivo*, oral administration of ISL significantly inhibited the MV4-11 flank tumor growth and prolonged the survival in the bone marrow transplant model via decreasing the expression of Ki67, and inducing apoptosis. Taken together, the present study identified a novel function of ISL as a selective FLT3 inhibitor. ISL could also be a potential natural bioactive compound for treating AML with FLT3-ITD or FLT3-ITD/F691L mutations. Thus, ISL and licorice might possess potential therapeutic effects for treating AML, providing a new strategy for anti-AML.

Keywords: Isoliquiritigenin, AML, FLT3, FLT3-ITD/F691L, Licorice

Molecular Pharmacology Fast Forward. Published on August 28, 2019 as DOI: 10.1124/mol.119.116129
This article has not been copyedited and formatted. The final version may differ from this version.

Introduction

Acute myeloid leukemia (AML) is the most frequently diagnosed type of aggressive hematological malignancy in adults with more than 20,000 newly diagnosed patients in America every year (Siegel *et al.*, 2015). Although the mortality has substantially declined over the past two decades with the implementation of therapeutic modalities of standard chemotherapy, chemotherapy resistance and intolerance are inevitable (Döhner *et al.*, 2017; Podoltsev *et al.*, 2017). Consequently, the identification and development of safer and more effective anti-AML agents are highly desirable.

The high relapse rates of AML may be attributed partially to genetic and epigenetic heterogeneity and chemoresistance-enabling mutations (Papaemmanuil *et al.,* 2016; Tsai *et al.*, 2016). Moreover, nearly 30% of AML patients carry activating mutations in the FMS-like tyrosine kinase-3 (FLT3) gene which encodes a class III receptor tyrosine kinase and regulates the normal hematopoiesis (Gilliland *et al.,* 2002; Prada-Arismendy *et al.*, 2017). The accumulated evidence over the past years indicated that internal tandem duplication mutations in juxtamembrane domain of FLT3 kinase (FLT3-ITD) are the most prevalent mutations that lead to uncontrolled cellular proliferation and survival characterized by constitutive ligand-independent activation of FLT3 (Kiyoi *et al*., 2002; Levis *et al.*, 2018). Several studies have demonstrated that patients with high FLT3-ITD allelic ratios exhibit a high relapse rate, poor prognosis, and worse survival rate (El Fakih *et al.,* 2018; Döhner *et al.,* 2017). Recently, small-molecule FLT3 inhibitor, Midostaurin

Molecular Pharmacology Fast Forward. Published on August 28, 2019 as DOI: 10.1124/mol.119.116129
This article has not been copyedited and formatted. The final version may differ from this version.

has been demonstrated to effectively inhibit the growth of FLT3-ITD-positive AML cells in animal and human, and has been approved by USFDA for treating AML (Stone *et al.*, 2017). Moreover, a number of small-molecule FLT3 inhibitors, including Quizartinib (Cortes *et al.*, 2018), Sunitinib (Fiedler *et al.*, 2015), Ponatinib (Shah *et al.*, 2013), MLN-518 (Odia *et al.*, 2016) and Gilteritinib (Perl *et al.*, 2017) are being studied in the clinical trials, and have yielded favorable results against AML FLT3-ITD mutant isoforms. Although these FLT3 inhibitors exhibit potent anti-AML activity in clinical trials, drug resistance and relapse often occur. Recently, point mutational analysis showed that F691L mutation in tyrosine kinase domain (TKD) of FLT3-ITD confer acquired resistance to these drugs (Albers *et al.*, 2013; Xu *et al.*, 2017). Thus, acquired resistance is still a challenge in the drug development of FLT3 targeted therapy.

Isoliquiritigenin (ISL), a natural flavonoid mainly extracted from licorice root, is one of the most widely used traditional Chinese medicines in China, and is often used in food flavoring in Western countries. Previous studies have demonstrated that ISL possesses various pharmacological action, including anti-inflammatory (Zeng *et al.*, 2017), anti-platelet aggregation (Tawata *et al.*, 1992), spasmogenic (Liu *et al.*, 2008), antimicrobial (Boyapelly *et al.*, 2017), vasorelaxant (Yu *et al.*, 1995), and estrogenic effects (Kundu *et al.*, 2018). Moreover, ISL has been proved to possess significant inhibitory activities against liver (Hsu *et al.*, 2005), colon (Wu *et al.*, 2016), prostate (Zhang *et al.*, 2016a), and cervical cancer cells via inducing apoptosis or autophagy, cell

Molecular Pharmacology Fast Forward. Published on August 28, 2019 as DOI: 10.1124/mol.119.116129
This article has not been copyedited and formatted. The final version may differ from this version.

cycle arrest, or inhibiting migration and triggering oxidative stress (Tsai *et al.*, 2015; Peng *et al.,* 2015). Previously, our group demonstrated that ISL exhibited a significant inhibitory effect on breast cancer through suppressing angiogenesis, repressing cancer stem cells, regulating autophagy, and modulating miR-374a (Wang *et al.*, 2013; Wang *et al*., 2014; Wang *et al*., 2015; Peng *et al.*, 2017). These results suggested that ISL is a multifunctional natural bioactive compound with potent anticancer activities. However, there is little literature on the role and targets of ISL in human AML.

The results of our present study demonstrated that ISL could selectively inhibit the activation of the FLT3 kinase, and the viability of FLT3-ITD mutant AML cell lines with negligible activity in other types of tumor cells and normal cells *in vitro*. Furthermore, ISL could significantly inhibit tumor growth of MV4-11 in xenograft tumor model and bone marrow model with good tolerance. Taken together, the present study identified a novel function of ISL as a selective FLT3 inhibitor as well as a potential natural bioactive compound for treating AML with FLT3-ITD mutations.

Molecular Pharmacology Fast Forward. Published on August 28, 2019 as DOI: 10.1124/mol.119.116129
This article has not been copyedited and formatted. The final version may differ from this version.

Materials and methods

Materials

For the present study, 3-(4,5-dimethylthiazol-2-yl)-2,5-diphenyltetrazolium (MTT), dimethyl sulfoxide (DMSO), PEG400 were procured from Sigma Chemical Co. (St. Louis, MO): Rabbit anti-phosphorylated-FLT3 (p-FLT3, Tyr969, #3463), Rabbit anti-FLT3 (8F2, #3462), Rabbit anti-phosphorylated-STAT5 (p-STAT5, Tyr105, #3827), Rabbit anti-STAT5 (#9363), Rabbit anti-phosphorylated-p44/42 MAPK (P-Erk1/2, Thr202/Tyr204, #4370), Rabbit anti-p44/42 MAPK (P-Erk1/2, #4695). Mouse anti-β-actin (#3700) was purchased from Cell Signaling Technology (Beverly, MA), while Rabbit anti-Caspase-3 (ab184787) was purchased from Abcam (Cambridge, MA, USA). Isoliquiritigenin, with a purity of more than 97%, was obtained from Alpha Aesar (MA, USA). Sunitinib was acquired from Nanjing Chemlin Chemical Industry Co. Ltd (Nanjing, Jiangsu). All of the chemicals used in this study were of analytical grade.

Cell culture

Unless otherwise stated, the cell lines were obtained from the American Type Culture Collection (Manassas, VA, USA). All the cells except for MV4-11 cells were grown in RPMI 1640 or DMEM culture medium supplemented with 10% fetal bovine serum (v/v), 100U/ml penicillin, and 100U/ml streptomycin. MV4-11 cells were cultured in the

Molecular Pharmacology Fast Forward. Published on August 28, 2019 as DOI: 10.1124/mol.119.116129
This article has not been copyedited and formatted. The final version may differ from this version.

IMDM culture medium containing 10% fetal bovine serum (v/v) and antibiotics. All cultures were maintained at 37°C and 5% CO_2.

Cell viability assays

Cell viability was measured with the colorimetric MTT metabolic activity assay. Briefly, the leukemic cells were seeded in a 96-well plate at a density of $1\sim4\times10^4$ cells per well for 24 hrs and an equal volume of medium containing an increasing concentration of inhibitors was added to each well. The other cell lines were seeded in 96-well plates at a density of $2\sim5\times10^3$ cells/well for 24 hours and then the medium was replaced with the medium containing serial dilutions of inhibitors. After 72 hours of further incubation, 20 μL of 5 mg/mL MTT reagent was added into each well followed by 2-4 hours of incubation. Subsequently, 50 μL of 20% acidified SDS per well was added to lyse the cells. The absorbance values of the dissolved cells were measured at 570 nm with a SpectraMAX M5 microplate spectrophotometer (Molecular Devices). All experiments were performed in triplicate. Cell viability was calculated as the percentage of viable cells relative to the control cells treated with DMSO (0.1%).

***In vitro* kinase assay**

The recombinant human protein FLT3 was obtained from Eurofins. The inhibition of the FLT3 kinase activity was measured with homogeneous, time-resolved fluorescence (HTRF) assays. Optimal enzyme and substrate concentrations were determined with the

Molecular Pharmacology Fast Forward. Published on August 28, 2019 as DOI: 10.1124/mol.119.116129
This article has not been copyedited and formatted. The final version may differ from this version.

HTRF KinEASE kit (Cisbio, France) according to the manufacturer's instructions. Briefly, the FLT3 enzymes were mixed with peptide substrate in a kinase reaction buffer system containing 50 mM (pH7.0) HEPES, 0.02% NaN_3, 0.1 mM sodium orthovanadate, 5mM $MgCl_2$, 0.01% (w/v) bovine serum albumin (BSA), 1 μM TK substrate-biotin, and 2 μM ATP. The final concentration of the FLT3 in the system was 6 nM. The reaction was quenched by addition of development reagent, followed by incubation for an additional hour prior to fluorescence measurements on EnVision® Multilabel Reader (Perkin Elmer). Protein kinase profiling of ISL was also evaluated with HTRF assay in a panel of 5 human protein kinases. The percentage inhibition was calculated relative to an enzyme control without inhibitor. IC_{50} values were calculated by four-parameter non-linear regression analysis of the resulting concentration-response curves using GraphPad PRISM.

Enzyme kinetic experiments

To investigate whether the ATP binding site is the binding site of ISL with FLT3, the enzyme kinetic experiments were performed with the increasing concentration of ATP (0.16μM to 200 μM) in the kinase assay mentioned earlier.

Cell cycle analysis

For cell cycle analysis, MV4-11 cells were seeded into 6-well plates at a cell density of $2*10^5$/well. After 30 minutes, cells were treated with different concentrations of ISL

Molecular Pharmacology Fast Forward. Published on August 28, 2019 as DOI: 10.1124/mol.119.116129
This article has not been copyedited and formatted. The final version may differ from this version.

(0.625, 2.5 and 10 μM) for 20 hrs. The cells were harvested and washed in cold PBS. Then, the cells were fixed with 95% ice-cold ethanol and treated with RNase A (100 μg/ml) and stained with propidium iodide (PI; 10 μg/ml). Cell cycle distribution was analyzed by a flow cytometry (BD Biosciences).

Cell apoptosis

For cell apoptosis analysis, Annexin V-fluorescein isothiocyanate (FITC) apoptosis detection kit (KeyGen BioTECH) was used. Briefly, the MV4-11 cells were seeded into 6-well plates at a cell density of 1×10^6/well. After 30 minutes, cells were treated with different concentrations of ISL (2.5, 10, and 40 μM) for 30 hrs. The cells were washed twice with cold phosphate buffered saline (PBS), and then incubated with Annexin V-FITC/PI at RT for 5 mins in the dark. The fluorescence of the cells was detected by flow cytometry by using a FITC signal detector and a PI signal detector (BD Biosciences, USA).

The level of apoptosis was also analyzed by detecting the level of cleaved caspase-3. Briefly, MV4-11 cells were treated with ISL at indicated concentrations for 30 hours, and the cells were subsequently lysed with RIPA buffer (10 mM Tris-HCl (pH 7.8), 1% NP40, 0.15 M NaCl, 1 mM EDTA, 10 μM aprotinin, 1 mM NaF and 1 mM Na_3VO_4). The extracted samples were subjected to Western analysis as described below using an anti-caspase 3 antibody and GAPDH as the control.

Molecular Pharmacology Fast Forward. Published on August 28, 2019 as DOI: 10.1124/mol.119.116129
This article has not been copyedited and formatted. The final version may differ from this version.

Western blot analysis

Cells (MV4-11) were treated with a series of concentrations of ISL and harvested after 20 hrs, then washed with pre-cooled PBS. Total protein was extracted in ice-cold RIPA lysis (10 mM Tris-HCl (pH 7.8), 1% NP40, 0.15 M NaCl, 1 mM EDTA, 10 μM aprotinin, 1 mM NaF and 1 mM Na3VO4). Protein concentration was determined using BCA protein quantification assay kit. For western blot assay, the proteins were resolved with 10-15% SDS-PAGE gel electrophoresis followed by transfer to PVDF membranes (Millipore, Billerica, MA, USA) and incubated overnight with the appropriate antibodies. Primary antibodies against FLT3/p-FLT3, STAT5/p-STAT5, Erk1/2/p-Erk1/2 and β-actin were used to probe with proteins on the membrane at 4℃ overnight. Subsequently, the membranes were washed three times with TBST (Tris-buffered saline with tween) and incubated with horseradish peroxidase (HRP)-conjugated secondary antibody for 2 hrs at room temperature. Specific antibody binding was detected by electrochemiluminescence (ECL) kit on Kodak X-ray films.

Computational Docking Studies

Comparative receptor structure models for the FLT3/F691L, a point mutation of FLT3 were generated with the 'Build Mutants' module of Discovery Studio (DS) 3.1 (Accelrys, Inc., USA) program package. Molecular docking studies were performed using the co-crystal structures of FLT3 with the AC220 (Quizartinib, a type II kinase inhibitor) as templates to build the receptor structure of point mutations. The best set of parameters in

Molecular Pharmacology Fast Forward. Published on August 28, 2019 as DOI: 10.1124/mol.119.116129
This article has not been copyedited and formatted. The final version may differ from this version.

the DS 3.1 program identified during parameter optimization comprises the following settings: parameter value of mutant was set as PHE691LEU. Input protein molecule was set to 4XUF, a number of models were set to 5, optimization level was set to high and other parameters were set as 'Build Mutants Default'.

GOLD (Genetic Optimization for Ligand Docking) can dock flexible ligands into a protein active site based on the genetic algorithm. Thus, GOLD was used for docking studies and all the GOLD protocols were executed in the program package of DS3.1. The Docking calculations were set to add hydrogen in the homology modeling of 4XUF.M0005 and define the receptor for 4XUF.M0005. Then, the binding site containing the ligand of AC220 was defined as an active sphere whose radius was set to 9 Å in this crystal structure. The default calculation mode which provided the best-docked results was selected for calculation~~s~~.

Effect of ISL on AML cell growth *in vivo*

Seven to eight-week-old female NOD/SCID mice were obtained and housed in a sterile environment and fed a standard diet *ad libitum*. The animals were cared for in accordance with the Guide for the Care and Use of Laboratory Animals of the National Institutes of Health. To establish the AML xenograft model, single-cell suspensions of MV4-11 (6×10^7 cells/ml) in serum-free medium were injected into the hind flank at 100 μl/site. When the tumors reached a size of 100~200 mm^3, the mice bearing tumors were equally divided into different groups (6 mice each group) and received oral dose of ISL (25, 50,

and 100 mg/kg/day p.o., respectively) or vehicle (5% DMSO+20% PEG400+75% normal saline) for 18 days. Positive control group mice were injected with sunitinib (10 mg/kg/day p.o.). Tumors growth and body weight were measured every 3 days with a Vernier caliper during the treatment *in vivo*, and the tumor volume was calculated using the following formula: volume (mm^3) = $a \times b^2/2$ (a, longest diameter (length); b, shortest diameter (width)). The mice were closely monitored and weighed. At the end of the experiment, animals were euthanized, and the tumors were harvested and subjected to histological examination.

Effect of ISL in the bone-marrow engraftment model

NOD-SCID mice were pretreated with cyclophosphamide at a dose of 150 mg/kg i.p. once a day for 2 days. After 24-hours, each mouse was intravenously injected with 5×10^6 MV-4-11 cells via the tail vein. After 20 days of inoculation, ISL or vehicle was administered orally once a day for 30 days. Positive control group mice were injected with sunitinib (10 mg/kg/day). Survival was determined by observation of the animals without hind-limb paralysis and those that were moribund were counted as dead.

Immunohistochemistry

Tumor samples obtained from *in vivo* studies were rinsed, fixed with 10% paraformaldehyde/PBS and embedded in paraffin. The femoral bones of bone-marrow engrafted mice were fixed, decalcified, and embedded in paraffin. For

Molecular Pharmacology Fast Forward. Published on August 28, 2019 as DOI: 10.1124/mol.119.116129
This article has not been copyedited and formatted. The final version may differ from this version.

immunohistochemical analysis, paraffin-embedded tumors were sectioned (4-8 um) and subjected to immunostaining with Ki67. Furthermore, apoptosis was detected by TUNEL (transferase-mediated dUTP nick-end labeling) assay as described by the manufacturer. Briefly, deparaffinized sections were permeabilized with 0.1% Triton X-100 solution and then incubated with 50 μl TUNEL reaction mixture at 37℃ for 60 mins. After rinsing thrice with PBS, 50 μl Converter-POD was added and the tissue cells were incubated for 30 mins at 37℃. Subsequently, the sections were stained using DAB substrate and counterstained with hematoxylin. Apoptotic cells were then visualized with a Leica digital camera attached to a light microscope.

Statistical analysis

All in vitro experiments were performed in triplicate and replicated more than three times. The data was expressed as means ± standard deviations (SD). Student t-test was used to compare the differences between two groups; for multiple comparison, a post-hoc test using Dunnett's method was used to assess the differences between the treated groups and control group; to assess the survival rate of mice, a Kaplan-Meier curve was performed. All the statistical analyses were conducted using GraphPad Prism (version 5.01). The value $p < 0.05$ was considered to be statistically significant.

Molecular Pharmacology Fast Forward. Published on August 28, 2019 as DOI: 10.1124/mol.119.116129
This article has not been copyedited and formatted. The final version may differ from this version.

Results

In the vitro growth inhibitory activity of ISL against leukemia and other cell lines

The *in vitro* growth inhibitory activities of ISL were evaluated against a panel of tumor cell lines, including leukemia and solid tumor cell lines. As presented in Table 1, ISL selectively inhibited the viability of FLT3-ITD mutant AML cell lines including MV4-11 and MOLM-13 in a dose-dependent manner with IC_{50} values of 3.2 ± 1.2 μM (0.85 ± 0.32 μg/ml), and 4.9 ± 2.1 μM, respectively. However, a relatively weak inhibitory activity was observed in human B cell lymphoma cell lines (OCI-LY10; IC_{50}: 20.1 ± 6.7 μM). Negligible activity was detected against the normal human epithelial mammary cell line MCF-10A and other human common solid tumor cell lines (Table 1). These results indicated that AML cells with FLT3-ITD mutant were extremely sensitive to ISL than other cell lines tested.

Inhibitory effect of ISL on FLT3 and kinase selectivity

In vitro, enzyme kinetics assay revealed a remarkable inhibitory effect of ISL on FLT3 at the nanomolar concentration with IC_{50} value of 115.1 ± 4.2 nM. The inhibitory effect of ISL on tyrosine kinase EGFR was noticeably weak with IC_{50} value of 16.19 ± 2.4 μM. Conversely, ISL was largely inactive against tyrosine kinase BTK (IC_{50}>20 μM). Meanwhile, ISL was highly selective for various types of Ser/Thr kinases including

Molecular Pharmacology Fast Forward. Published on August 28, 2019 as DOI: 10.1124/mol.119.116129
This article has not been copyedited and formatted. The final version may differ from this version.

CHK1, AKT1, and Aurora-A with IC_{50} values of >20μM, 19.0 ± 3.8μm, and 8.7 ± 0.9μm, respectively. These data suggested that ISL was a highly selective inhibitor of FLT3 (Fig.1B). In addition, the enzyme kinetic experiments were conducted with a different concentration of ATP (0.16 μM to 20 μM). With the increased concentration of ATP, the IC_{50} value of ISL to FLT3 also increased considerably from 20.0 ± 7.3 nM to 430.9 ± 47.8 nM, demonstrating that ISL was an ATP-competitive FLT3 inhibitor (Fig. 1C and D).

Selective inhibition of proliferation of Ba/F3-FLT3-ITD cells by ISL

Next, ISL was tested for the ability to selectively induce cell death in growth factor-independent Ba/F3-FLT3-ITD cells, without affecting parental, growth factor (IL-3)-dependent murine pro-B cell line Ba/F3. As shown in Fig 1E, ISL significantly inhibited the proliferation of Ba/F3-FLT3-ITD cells at various concentrations between 2.5 and 40 μM with an IC_{50} value of 2.9 ± 0.8 μM within 72 hrs and was nontoxic toward parental Ba/F3 cells at concentrations up to 40 μM. However, Ba/F3-FLT3-ITD cells could be rescued from the anti-proliferative effects of ISL by IL-3. This data suggested that ISL selectively inhibited the cell growth by targeting FLT3 and did not inhibit any other kinases in the signaling pathways used by the IL-3 receptor in Ba/F3 cells.

FLT3-ITD/TKD (ITD plus F691L) dual mutation remains the main cause of the development of resistance to the FLT3 inhibitor. Among them, FLT3-ITD F691L mediated a noticeable strong resistance towards the FLT3 inhibitors, AC220, and

Molecular Pharmacology Fast Forward. Published on August 28, 2019 as DOI: 10.1124/mol.119.116129
This article has not been copyedited and formatted. The final version may differ from this version.

sorafenib. We performed proliferation studies of ISL on Ba/F3 cells expressing FLT3-ITD/F691L and confirmed that ISL exhibited the ability to inhibit the proliferation of Ba/F3-FLT3-ITD/F691L with an IC_{50} value of 5.5 ± 1.9 μ M, and Ba/F3-FLT3-ITD/F691L cells were also rescued by IL-3 (Fig 1F). AC220 and sorafenib are very effective in inhibiting the proliferation of Ba/F3-FLT3-ITD cells, but they don't have an ideal effect on BA/F3-FLT3-ITD/F691L cells (Fig 1G and H). These findings suggested that ISL could be utilized as a clinically active compound in patients with FLT3-ITD mutation and patients with acquired FLT3-ITD/TKD dual mutation.

Predicted binding mode of ISL with FLT3.

In order to investigate the possible binding mode of ISL with FLT3, the computational molecular docking studies were carried out using Discovery Studio (DS) 3.1 program package. The molecular docking studies were based on the known co-crystal structure of FLT3 with its inhibitor quizartinib (AC220) (PDB code 4XUF) (Zorn et al., 2015; Smith et al., 2015), and the binding mode of bioactive compound ISL with FLT3 was presented in **Fig. 2**. The carbonyl group and 4λ^3-benzene-1,3-diol group of ISL were hydrogens bonded with CYS694. Besides, the other two hydrogen bonds were also formed in 4λ^3-phenol group with LYS644 and ASP829. Furthermore, one face-to-face sigma-π interaction was formed, which was between the hydrogen atom in the 4λ^3-phenol group and the benzene ring of PHE830. ISL also formed a hydrophobic interaction with

Molecular Pharmacology Fast Forward. Published on August 28, 2019 as DOI: 10.1124/mol.119.116129
This article has not been copyedited and formatted. The final version may differ from this version.

residues LEU818, PHE691, PHE830, VAL624, and TYR693 in ATP binding pocket of FLT3.

To illustrate the underlying mechanism of how ISL retains its activity against the F691L mutation, the protein models of point mutation of FLT3/F691L were established. They were based on the co-crystal structure of FLT3 bound to AC220 (PDB entry 4XUF 4XUF) as a template by defining the 'Build Mutants' module in Discovery Studio (DS) 3.1 program package. Five different protein models of point mutations were obtained after running the DS 3.1 program. The sequence was represented in tabular form according to their PDF total energy from low to high (See Table 2). PDF total energy of 4XUF.M0005 was recorded to be 1215.7684, which was relatively lower than other energy of the protein model. Thus, 4XUF.M0005 was selected as a receptor to further investigate the binding mode of ISL with the F691L mutation. From Fig. 2, it was revealed that the binding mode exhibited lower homology with the binding mode of ISL with FLT3; the stable combined conformation revealed that ISL could overcome the mutation of FLT3/F691L.

ISL induces G0-G1 phase arrest and apoptosis in AML cells

Measurement of cellular DNA content and the analysis of the cell cycle were performed by flow cytometry. The cells were treated with different concentrations of ISL (0.625, 2.5 and 10μM) for 20 hrs, and the levels of cell cycle progression were examined by flow cytometry. ISL significantly increased the number of MV4-11 cells in G1 phase. The

Molecular Pharmacology Fast Forward. Published on August 28, 2019 as DOI: 10.1124/mol.119.116129
This article has not been copyedited and formatted. The final version may differ from this version.

amount of cells in the G1 phase was increased from 52.52% to 66.70% (Fig 3A and 3C.). In contrast, ISL markedly decreased the number of cells in S phase and G2/M in a dose-dependent manor, with the percentage decrease from 32.16% to 23.36% in S phase and 16.55% to 6.47% in G2/M, respectively. These results suggested that ISL could induce G0-G1 phase arrest in MV4- 11 cells.

ISL induces apoptotic cell death

Next, we investigated apoptotic cell death using Annexin V-FITC assay. With the increasing concentration of ISL, the proportion of MV4-11 cells in the apoptosis increased significantly from 3.92 ± 2.65% to 53.11 ± 11.31% (Fig. 3B and 3D). For determination of the apoptotic pathway, we measured the expression of proteins involved in apoptosis by western blotting. The concentration of ISL increased (2.5, 10, and 40 μM), and the cleavage of Caspase 3 increased significantly too (Fig. 4B). These results indicated that ISL could induce apoptosis in a dose-dependent manner, at concentration above the IC_{50} value in AML cells.

Targeting of FLT3 signaling pathways by ISL in AML cells

To determine the ability of ISL in blocking FLT3 and its downstream signaling, we screened some essential kinases involved in FLT3 signaling pathway using Western blot analysis. After a 20-hour treatment with gradient concentrations of ISL, MV4-11 cells were harvested and lysed for an immunoblot assay. As shown in Fig.4A, ISL significantly

Molecular Pharmacology Fast Forward. Published on August 28, 2019 as DOI: 10.1124/mol.119.116129
This article has not been copyedited and formatted. The final version may differ from this version.

suppressed the auto-phosphorylation of FLT3-ITD in a dose-dependent manner. Downstream signaling proteins Erk1/2 and STAT5 were also strongly inhibited by ISL at concentration of ≥ 5 μM. Similarly, sunitinib (positive control) also inhibited the phosphorylation of FLT3, Erk1/2, and STAT5 in MV4-11 cells. Moreover, ISL did not interfere with the expression of these proteins during the treatment period. These findings suggested that ISL exerted its anti-AML function by directly targeting FLT3 displayed on the surface of leukemic cells and further antagonizing FLT3-mediated downstream signaling cascade.

In vivo effects of ISL against MV4-11 tumor xenografts

The *in vivo* anti-AML activity of ISL was evaluated in the MV4-11 tumor xenograft model of NOD-SCID mice. The xenograft-bearing animals were treated orally with different doses of ISL at 100 mg/kg/day, 50 mg/kg/day and 25 mg/kg/day or with vehicle alone. Oral sunitinib at a dose of 10 mg/kg/day was used as positive control. As shown in Fig. 5A, treatment with ISL for 18 days exhibited a significant antitumor activity and inhibited MV4-11 tumor progression as compared with the vehicle group. Treatment with ISL at a dose of 100 mg/kg/day and treatment with sunitinib at 10 mg/kg/day elicited maximum tumor inhibition rates of 83.2% and 84.9% respectively when compared with the vehicle-treated mice. ISL at doses of 50 mg/kg/day and 25 mg/kg/day also significantly inhibited the MV4-11 tumor growth with anti-tumor rates of 60.3% and 46.8% respectively. The body weight of mice was monitored once every 3 days during

the course of the experiment. As illustrated in Fig. 5B, no significant loss in the body weight was observed between the ISL treated and vehicle-treated group. No significant differences in gross measures including skin ulcerations or toxic death were observed in ISL-treated mice. Meanwhile, Shoji Yamazaki et al proved that isoliquiritigenin (intraperitoneal injection) had a LD_{50} of about 3000 mg/kg in mice and did not cause animal death at 2000 mg/kg (Yamazaki et al., 2002). These data indicated that ISL inhibited the AML tumor growth in vivo without systemic toxicity.

In addition, the *in vivo* expression of p-Erk1/2 and Ki67 were measured by western blots and immunohistochemical analysis. As shown in Fig. 5D, the percentage of Ki67-expressing and p-Erk1/2 positive cells in ISL-treated tumor tissue were significantly lower than vehicle-treated tumor tissue. Meanwhile, the results of western blots also corroborated that ISL could inhibit the *in vivo* expression of p-Erk1/2 and Ki67 (Fig 5E). The Ki-67 protein expression was an established prognostic factor and was extensively used in the routine pathological investigation as a proliferation marker or as a cell mitotic index. Furthermore, TUNEL assay were used to detect the *in vivo* cell apoptosis induced by ISL. As illustrated in Fig. 5D, tissue sections from the 100 mg/kg ISL-treated group possessed more TUNEL-positive cell, indicating a tumor with more apoptotic cells. These results demonstrated that ISL inhibited AML cells proliferation and induced apoptosis *in vivo*.

Molecular Pharmacology Fast Forward. Published on August 28, 2019 as DOI: 10.1124/mol.119.116129
This article has not been copyedited and formatted. The final version may differ from this version.

Evaluation of survival in a bone marrow model

To evaluate the influence of ISL on the survival time, we established a bone marrow engraftment model that mimics the pathology of human leukemia. MV4-11 cells were intravenously engrafted into mice after their endogenous bone marrow was ablated by pretreatment with cyclophosphamide. After allowing the disease to establish for 20 days, the mice were randomly divided into different groups (10 mice each group), and treatment was initiated with 50, 100 mg/kg/d ISL or with vehicle alone. Sunitinib at a dose of 10 mg/kg/d was used as a positive control. All vehicle group mice were presented with hind-limb paralysis or moribund within 42 to 60 days with a mean survival time (MST) of 52 days. The sunitinib-treated mice exhibited an MST of 70 days, and all animals expired by day 77. ISL-treated mice demonstrated prolonged survival in a dose-dependent manner; the MSTs determined to be 60 and 68 days for the 50 and 100 mg/kg/d groups respectively (Fig. 5C). In addition, we also determined the number and activity of MV4-11 cells in bone marrow. As shown in Fig. 5F, bone marrow MV4;11 cells in vehicle group exhibited a strong nuclear immunoreactivity for Ki67, while other cells stained weakly. Treatment with ISL at 100 mg/kg/d resulted in reduced numbers of bone marrow MV4-11 cells when examined on day 40. In some cases of treatment with ISL, only a few leukemic cells distributed throughout the bone marrow remained. These findings suggested that ISL exhibited high efficacy in an FLT3-ITD model of lethal bone marrow disease in a dose-dependent manner to the subcutaneous.

Molecular Pharmacology Fast Forward. Published on August 28, 2019 as DOI: 10.1124/mol.119.116129
This article has not been copyedited and formatted. The final version may differ from this version.

Discussion

AML is the most heterogeneous hematological malignancy associated with a low survival rate in adults. Over the past few decades, tremendous technical advances in the cytogenetic analysis have been made for early diagnosis and prognostic stratification. However, chemotherapy and hematopoietic stem cell transplantation remain the predominant treatment methods for AML, yet with a low five-year survival rate (20%) of AML patients (Ottmann *et al*., 2018; Schlenk *et al.*, 2014). Related research has shown that the survival rate of the patients using TCM is considerably higher than that of TCM nonusers (Huang *et al.*, 2017). Particularly, the treatment with As_2O_3 is highly effective in AML patient with resistance to ATRA and chemotherapy with relatively better safety (Wang *et al.*, 2008; Li *et al.*, 2017). Thus, traditional Chinese drugs may have potential therapeutic effects on AML.

Licorice, name derived “gancao” in China, is a very well-known herb in traditional Chinese medicine. It has been used for centuries and can be dated back to the Shen nong's Classic of Materia Medica around 2100 BC (Gibson *et al.*, 1978). During the following millennia, licorice roots have been used for treating diseases like influenza, coughs, liver damage and for detoxification (Kao *et al.*, 2014). Recently, pharmacological studies have revealed numerous biological activities associated with licorice, such as anti-viral, anti-diabetic, anti-inflammatory, anti-tumor, anti-microbial, cholinergic regulation, and many more (Bode *et al*., 2015). Consequently, over 400 chemical components have been

Molecular Pharmacology Fast Forward. Published on August 28, 2019 as DOI: 10.1124/mol.119.116129
This article has not been copyedited and formatted. The final version may differ from this version.

extracted and separated from licorice, containing nearly 300 flavonoids (Ji *et al*., 2016). However, the effective components in licorice responsible for these bioactivities remain elusive. Therefore, identification of their potential activity deserves more attention for development of the novel drug.

Isoliquiritigenin, a natural flavonoid constituent of licorice, possesses various medicinal bioactivities, including neuroprotective (Yang *et al.*, 2016), analgesic (Shi *et al.*, 2012), cardiac protection (Zhang *et al.*, 2016), and anti-inflammatory properties (Zhang *et al.*, 2018). There is a lot of evidence showing ISL has significant anti-tumor activity against many kinds of tumors, such as lung, colon, prostate, breast, gastric and cervical cancer. It has also been shown to inhibit the VEGF/VEGFR-2 signal (Wang *et al.*, 2013), suppress the activity of COX-2 (Zhang *et al*., 2014), increase CDK2 activity (Ii et al., 2004), and trigger ROS in cancer cells (Kim *et al*., 2017). However, the anti-AML activities of ISL remain to be completely elucidated. Furthermore, potential targets of ISL are also largely unknown. Therefore, the present study aimed to investigate the anti-AML activity of ISL. We found that ISL could selectively inhibit FLT3-ITD mutant AML cells via targeting FLT3.

In vitro, ISL selectively inhibited the proliferation of FLT3-ITD mutant AML cell lines, including MV4-11 and MOLM-13 with IC_{50} values of 0.85 ± 0.32 μg/mL, 1.27 ± 0.53 μg/mL and exhibited weak toxicity effects or negligible activity in other tumor cell lines and normal cells. Moreover, ISL significantly inhibited the tumor growth of MV4-11

Molecular Pharmacology Fast Forward. Published on August 28, 2019 as DOI: 10.1124/mol.119.116129
This article has not been copyedited and formatted. The final version may differ from this version.

xenograft model *in vivo*, and significantly prolonged the survival time in mice bone marrow AML model with better tolerance. Kinase profile data indicated that FLT3 was a selective target for ISL. Immunoblot assay revealed that ISL could effectively inhibit the phosphorylation of FLT3/Erk1/2/STAT5 signaling pathway within 20 hours but did not regulate the expression of these proteins. Notably, ISL still retained a good inhibitory activity against FLT3-ITD/F691L mutation, a resistance kinase domain mutation against well-known FLT3 inhibitor, sorafenib and AC220. These results indicated that ISL could be a promising novel bioactive lead compound for AML treatment.

FLT3 is one of the most crucial drug targets in AML, because patients carrying FLT3-ITD mutations have poor response to standard chemotherapy and inflict approximately 30% of cases AML with poor prognosis (Gilliland *et al.*, 2002; Prada-Arismendy *et al*., 2017). FLT3 inhibitors, including Midostaurin (Stone *et al.*, 2017), Quizartinib(AC220) (Cortes et al., 2018), Ponatinib (Shah *et al.*, 2013), and MLN-518 (Odia *et al*., 2016) have been demonstrated to inhibit the growth of FLT3-ITD-positive AML cells in animal and human. Conversely, a clinical study proved that FLT3-ITD-F691L mutation can cause acquired resistance to Quizartinib(AC220) and other FLT3 inhibitors (Albers *et al*., 2013). Thus, we conducted proliferation studies of ISL in Ba/F3-FLT3-ITD/F691L cells and confirmed significant inhibitory activity of ISL on FLT3-ITD/F691L cells which is similar to that of FLT3-ITD cells. These cells could all be rescued by IL-3. Thus, ISL could also be expected to be clinically active in patients with acquired FLT3-ITD/TKD dual mutations.

Molecular Pharmacology Fast Forward. Published on August 28, 2019 as DOI: 10.1124/mol.119.116129
This article has not been copyedited and formatted. The final version may differ from this version.

In summary, isoliquiritigenin is an orally available natural bioactive compound, exhibiting anti-AML efficacy via targeting FLT3 both *in vitro* and *in vivo*. Therefore, this novel FLT3 inhibitor has the potential to contribute to the treatment of recurrence of FLT3-ITD mutant AML. In tandem with other anti-AML drugs, ISL might exhibit an enhanced therapeutic outcome in AML.

Conflict of interest

The authors declare no conflicts of interests.

Acknowledgments

This study was supported by the National Natural Science Foundation of China (81873073, 81573663, 81503346, 81630101), International Science Foundation of Guganxi (AB16450008), National Major Scientific and Technological Special Project of China (2017ZX09201001-008), Youth Scientific Research Fund of CDUTCM (ZRQN1764, ZRQN1770), Sichuan Science and Technology Program (2018SZDZX0017).

Author contributions

ZX Cao., Y Wen and JL He. designed the studies, conducted most of the experiments, analyzed and interpreted the data, and wrote the manuscript. SZ Huang performed the computational docking studies. F Gao and QQ Liu contributed to the flow cytometry and kinase assay. CJ Guo., SW Zheng, DY Gong, YZ Li and RQ Zhang contributed to the western blot and animal studies. JP Chen and C Peng designed the studies, analyzed and

interpreted the data, and wrote the manuscript. All authors have read and approved the manuscript.

Reference

Albers C, Leischner H, Verbeek M, Yu C, Illert AL, Peschel C, von Bubnoff N and Duyster J (2013). The secondary FLT3-ITD F691L mutation induces resistance to AC220 in FLT3-ITD+ AML but retains in vitro sensitivity to PKC412 and Sunitinib. *Leukemia* 27: 1416-1418.

Bode AM and Dong Z (2015). Chemopreventive effects of licorice and its components[J]. *Curr Pharmacol Rep* 1: 60-71.

Boyapelly K, Bonin MA, Traboulsi H, Cloutier A, Phaneuf SC, Fortin D, Cantin AM, Richter M.V and Marsault E (2017). Synthesis and Characterization of a Phosphate Prodrug of Isoliquiritigenin. *J Nat Prod.* 80: 879-886.

Chen GQ, Shi XG, Tang W, Xiong SM, Zhu J, Cai X, Han ZG, Ni JH, Shi GY, Jia PM, Liu MM, He KL, Niu C, Ma J, Zhang P, Zhang TD, Paul P, Naoe T, Kitamura K, Miller W, Waxman S, Wang ZY, de The H, Chen SJ and Chen Z (1997). Use of arsenic trioxide (As2O3) in the treatment of acute promyelocytic leukemia (APL): I. As2O3 exerts dose-dependent dual effects on APL cells. *Blood* 89: 3345-3353.

Cortes J, Perl AE, Döhner H, Kantarjian H, Martinelli G, Kovacsovics T, Rousselot P, Steffen B, Dombret H, Estey E, Strickland S, Altman JK, Baldus CD, Burnett A, Krämer A, Russell N, Shah NP, Smith CC, Wang ES, Ifrah N, Gammon G, Trone D, Lazzaretto D and Levis M (2018). Quizartinib, an FLT3 inhibitor, as monotherapy in patients with relapsed or refractory acute myeloid leukaemia: an open-label, multicentre, single-arm, phase 2 tria. *Lancet Oncol* 19: 889-903.

Döhner H, Estey E, Grimwade D, Amadori S, Appelbaum FR, Büchner T, Dombret H, Ebert BL, Fenaux P, Larson RA, Levine RL, Lo-Coco F, Naoe T, Niederwieser D, Ossenkoppele GJ, Sanz M, Sierra J, Tallman MS, Tien HF, Wei AH, Löwenberg B and Bloomfield CD (2017). Diagnosis and management of AML in adults: 2017 ELN recommendations from an international expert panel. *Blood* 129: 424–447.

El Fakih R., Rasheed W, Hawsawi Y, Alsermani M and Hassanein M (2018). Targeting FLT3 Mutations in Acute Myeloid Leukemia. *Cells* 7: E4.

Fiedler W, Kayser S, Kebenko M, Janning M, Krauter J, Schittenhelm M, Götze K, Weber D, Göhring G, Teleanu V, Thol F, Heuser M, Döhner K, Ganser A, Döhner H, Schlenk RF (2015). A phase I/II study of sunitinib and intensive chemotherapy in patients over 60 years of age with acute myeloid leukaemia and activating FLT3 mutations. *Br J Haematol* 169: 694-700.

Gibson MR (1978). Glycyrrhiza in old and new perspectives. Lloydia 41:348–54.

Gilliland DG and Griffin JD (2002). The roles of FLT3 in hematopoiesis and leukemia. *Blood* 100: 1532-1542.

Hsu YL, Kuo PL and Lin CC (200). Isoliquiritigenin induces apoptosis and cell cycle arrest through p53-dependent pathway in Hep G2 cells. *Life Sci* 77: 279-292.

Ii T, Satomi Y, Katoh D, Shimada J, Baba M, Okuyama T, Nishino H and Kitamura N (2004). Induction of cell cycle arrest and p21CIP1/WAF1 expression in human lung cancer cells by isoliquiritigenin. *Cancer Lett* 207: 27-35.

Huang L, Li H, Xie D, Shi T and Wen C (2017). Personalizing Chinese medicine by integrating molecular features of diseases and herb ingredient information: application to acute myeloid leukemia. *Oncotarget* 8: 43579-43591.

Ji S, Li Z, Song W, Liang W, Li K, Tang S, Wang Q, Qiao X, Zhou D, Yu S and Ye M (2016). Bioactive constituents of Glycyrrhiza uralensis (Licorice): Discovery of the effective components of a traditional herbal medicine. *J Nat Prod* 79: 281-292.

Kao TC, Wu CH and Yen GC (2014). Bioactivity and potential health benefits of licorice. *J Agric Food Chem* 62: 542-553.

Kim DH, Park JE, Chae IG, Park G, Lee S, Chun KS (2017). Isoliquiritigenin inhibits the proliferation of human renal carcinoma Caki cells through the ROS-mediated regulation of the Jak2/STAT3 pathway. *Oncol Rep* 38: 575-583.

Kiyoi H, Ohno R, Ueda R, Saito H and Naoe T (2002). Mechanism of constitutive activation of FLT3 with internal tandem duplication in the juxtamembrane domain. *Oncogene* 21:2555-2563.

Kundu P, Neese SL, Bandara S, Monaikul S, Helferich WG, Doerge DR, Khan IA and Schantz SL (2018). The effects of the botanical estrogen, isoliquiritigenin on delayed spatial alternation. *Neurotoxicol Teratol* 66: 55-62.

Levis MJ, Perl AE, Altman JK, Gocke CD, Bahceci E, Hill J, Liu C, Xie Z, Carson AR, McClain V, Stenzel TT and Miller JE (2018). A next-generation sequencing–based assay for minimal residual disease assessment in AML patients with FLT3-ITD mutations. *Blood Adv* 2: 825-831.

Li YZ, Yu S, Yan PA, Gong DY, Wu FL, He Z, Yuan YY, Zhao AY, Tang X, Zhang RQ, Peng C and Cao ZX (2017). Crotonoside exhibits selective post-inhibition effect in AML cells via inhibition of FLT3 and HDAC3/6. *Oncotarget* 8: 103087-103099.

Liu B, Yang J, Wen Q and Li Y (2008). Isoliquiritigenin, a flavonoid from licorice, relaxes guinea-pig tracheal smooth muscle in vitro and in vivo: role of cGMP/PKG pathway. *Eur J Pharmacol* 587: 257-266.

Odia Y, Sul J, Shih JH, Kreisl TN, Butman JA, Iwamoto FM and Fine HA (2016). A Phase II trial of tandutinib (MLN 518) in combination with bevacizumab for patients with recurrent glioblastoma. *CNS Oncol* 5: 59-67.

Ottmann OG, Müller-Tidow C, Krämer A, Schlenk RF, Lübbert M, Bug G, Krug U, Bochtler T, Voss F, Taube T, Liu D, Garin-Chesa P and Döhner H (2018). Phase I dose-escalation trial investigating volasertib as monotherapy or in combination with cytarabine in patients with relapsed/refractory acute myeloid leukaemia[J]. *Br J Haematol* doi: 10.1111/bjh.15204.

Papaemmanuil E, Gerstung M, Bullinger L, Gaidzik VI, Paschka P, Roberts ND, Potter NE, Heuser M, Thol F, Bolli N, Gundem G, Van Loo P, Martincorena I, Ganly P and Mudie L (2016). Genomic classification and prognosis in acute myeloid leukemia. *N Engl J Med* 374: 2209-2221.

Peng F, Du Q, Peng C, Wang N, Tang H, Xie X, Shen J and Chen J (2015). A review: the pharmacology of isoliquiritigenin. *Phytother Res* 29: 969-977.

Peng F, Tang H, Liu P, Shen J, Guan X, Xie X, Gao J, Xiong L, Jia L, Chen J and Peng C (2017). Isoliquiritigenin modulates miR-374a/PTEN/Akt axis to suppress breast cancer tumorigenesis and metastasis.*Sci Rep* 7: 9022.

Perl AE, Altman JK, Cortes J, Smith C, Litzow M, Baer MR, Claxton D, Erba HP, Gill S, Goldberg S, Jurcic JG, Larson RA, Liu C, Ritchie E, Schiller G, Spira

AI., Strickland SA, Tibes R, Ustun C, Wang ES, Stuart R., Röllig C, Neubauer A, Martinelli G, Bahceci E and Levis M (2017). Selective inhibition of FLT3 by gilteritinib in relapsed or refractory acute myeloid leukaemia: a multicentre, first-in-human, open-label, phase 1–2 study. *Lancet Oncol* 18: 1061-1075.

Podoltsev NA, Stahl M, Zeidan AM and Gore SD (2017). Selecting initial treatment of acute myeloid leukaemia in older adults. *Blood Rev* 31: 43-62.

Prada-Arismendy J, Arroyave JC and Röthlisberger S (2017). Molecular biomarkers in acute myeloid leukemia. *Blood Rev* 31: 63-76.

Schlenk RF, Kayser S, Bullinger L, Kobbe G, Casper J, Ringhoffer M, Held G, Brossart P, Lübbert M, Salih HR, Kindler T, Horst HA, Wulf G, Nachbaur D, Götze K, Lamparter A, Paschka P, Gaidzik VI, Teleanu V, Späth D, Benner A, Krauter J, Ganser A, Döhner H and Döhner K (2014). Differential impact of allelic ratio and insertion site in FLT3-ITD positive AML with respect to allogeneic hematopoietic stem cell transplantation. *Blood* 124:3441-3449.

Shah NP., Talpaz M., Deininger M.W.N., Mauro M.J., Flinn I.W., Bixby D., Lustgarten S., Gozgit J.M., Clackson T., Turner C.D., Haluska F.G., Kantarjian H., Cortes J.E., 2013. Ponatinib in patients with refractory acute myeloid leukaemia: findings from a phase 1 study. *Brit J Haematol* 162:548-552.

Shi Y, Wu D, Sun Z, Yang J, Chai H, Tang L and Guo Y (2012). Analgesic and uterine relaxant effects of isoliquiritigenin, a flavone from Glycyrrhiza glabra. *Phytother Res* 26: 1410-1417.

Siegel RL, Miller KD and Jemal A (2015). Cancer statistics, 2015. *CA Cancer J Clin* 65(1): 5–29.

Smith CC, Zhang C, Lin KC, Lasater EA, Zhang Y, Massi E, Damon LE, Pendleton M, Bashir A, Sebra R, Perl A, Kasarskis A, Shellooe R, Tsang G, Carias H, Powell B, Burton EA, Matusow B, Zhang J, Spevak W, Ibrahim PN, Le MH, Hsu HH, Habets G, West BL, Bollag G and Shah NP (2015). Characterizing and overriding the structural mechanism of the quizartinib-resistant FLT3 "gatekeeper" F691L mutation with PLX3397. *Cancer Discov* 5: 668-679.

Stone RM., Mandrekar SJ., Sanford BL., Laumann K, Geyer S, Bloomfield CD, Thiede C, Prior TW, Döhner K, Marcucci G, Lo-Coco F, Klisovic RB, Wei A, Sierra J, Sanz MA, Brandwein JM, de Witte T, Niederwieser D, Appelbaum FR, Medeiros BC, Tallman MS, Krauter J, Schlenk RF, Ganser A, Serve H, Ehninger G, Amadori S, Larson RA and Döhner H (2017). Midostaurin plus chemotherapy for acute myeloid leukemia with a FLT3 mutation. *N Engl J Med* 377(5): 454-464.

Tawata M, Aida K, Noguchi T, Ozaki Y, Kume S, Sasaki H, Chin M and Onaya T (1992). Anti-platelet action of isoliquiritigenin, an aldose reductase inhibitor in licorice. *Eur J Pharmacol* 212: 87-92.

Tsai CH, Hou HA, Tang JL, Liu CY, Lin CC, Chou WC, Tseng MH, Chiang YC, Kuo YY, Liu MC, Liu CW, Lin LI, Tsay W, Yao M, Li CC, Huang SY and Ko BS (2016). Genetic alterations and their clinical implications in older patients with acute myeloid leukemia. *Leukemia*, 2016, 30: 1485-1492.

Tsai JP, Lee CH, Ying TH, Lin CL, Lin CL, Hsueh JT, Hsieh YH (2015). Licochalcone A induces autophagy through PI3K/Akt/mTOR inactivation and autophagy suppression enhances Licochalcone A-induced apoptosis of human cervical cancer cells. *Oncotarget* 6: 28851-28866.

Wu M, Wu Y, Deng B, Li J, Cao H, Qu Y, Qian X and Zhong G (2016). Isoliquiritigenin decreases the incidence of colitis-associated colorectal cancer by modulating the intestinal microbiota. *Oncotarget*, 2016, 7: 85318-85331.

Wang N, Wang Z, Wang Y, Xie X, Shen J, Peng C, You J, Peng F, Tang H, Guan X and Chen J (2015). Dietary compound isoliquiritigenin prevents mammary carcinogenesis by inhibiting breast cancer stem cells through WIF1 demethylation. *Oncotarget* 6: 9854-9876.

Wang Z, Wang N, Han S, Wang D, Mo S, Yu L, Huang H, Tsui K, Shen J and Chen J. 2013. Dietary compound isoliquiritigenin inhibits breast cancer neoangiogenesis via VEGF/VEGFR-2 signaling pathway. *PloS one* 8 e68566.

Wang Z, Wang N, Liu P, Chen Q, Situ H, Xie T, Zhang J, Peng C, Lin Y and Chen J (2014). MicroRNA-25 regulates chemoresistance-associated autophagy in breast cancer cells, a process modulated by the natural autophagy inducer isoliquiritigenin. *Oncotarget* 5: 7013-7026.

Wang ZY and Chen Z (2008). Acute promyelocytic leukemia: from highly fatal to highly curable. *Blood* 111:2505-2515.

Xu B, Zhao Y, Wang X, Gong P and Ge W (2017). MZH29 is a novel potent inhibitor that overcomes drug resistance FLT3 mutations in acute myeloid leukemia. *Leukemia* 31: 913-921.

Yamazaki S, Morita T, Endo H, Hamamoto T, Baba M, Joichi Y, Kaneko S, Okada Y, Okuyama T, Nishino H and Tokue A (2002). Isoliquiritigenin suppresses pulmonary metastasis of mouse renal cell carcinoma. *Cancer letters* 183: 23-30

Yang EJ, Kim M, Woo JE, Lee T, Jung JW and Song KS (2016). The comparison of neuroprotective effects of isoliquiritigenin and its Phase I metabolites against glutamate-induced HT22 cell death. *Bioorg Med Chem Lett* 26: 5639-5643.

Yu SM and Kuo SC (1995). Vasorelaxant effect of isoliquiritigenin, a novel soluble guanylate cyclase activator, in rat aorta. *Br J Pharmacol* 114: 1587-1594.

Zeng J, Chen Y, Ding R, Feng L, Fu Z, Yang S, Deng X, Xie Z and Zheng S (2017). Isoliquiritigenin alleviates early brain injury after experimental intracerebral hemorrhage via suppressing ROS-and/or NF-κB-mediated NLRP3 inflammasome activation by promoting Nrf2 antioxidant pathway. *J Neuroinflammation* 14: 119.

Zhang B, Lai Y, Li Y, Shu N, Wang Z, Wang Y, Li Y and Chen Z (2016). Antineoplastic activity of isoliquiritigenin, a chalcone compound, in androgen-independent human prostate cancer cells linked to G2/M cell cycle arrest and cell apoptosis. *Eur J Pharmacol* 821: 57-67.

Zhang W, Tao Q, Guo Z, Fu Y, Chen X, Shar PA, Shahen M, Zhu J, Xue J, Bai Y, Wu Z, Wang Z, Xiao W and Wang Y (2016). Systems pharmacology dissection of the integrated treatment for cardiovascular and gastrointestinal disorders by traditional chinese medicine. *Sci Rep* 6: 32400.

Zhang W, Wang G and Zhou S (2018). Protective Effects of Isoliquiritigenin on LPS-Induced Acute Lung Injury by Activating PPAR-γ. *Inflammation* 41: 1290-1296.

Zheng H, Li Y, Wang Y, Zhang J, Chai H, Tang T, Yue J, Guo AM and Yang J (2014). Downregulation of COX-2 and CYP 4A signaling by isoliquiritigenin inhibits

human breast cancer metastasis through preventing anoikis resistance, migration and invasion. *Toxicol Appl Pharmacol* 280: 10-20.

Zorn JA, Wang Q, Fujimura E, Barros T and Kuriyan J (2015). Crystal structure of the FLT3 kinase domain bound to the inhibitor quizartinib (AC220). *PloS One* 10: e0121177.

Molecular Pharmacology Fast Forward. Published on August 28, 2019 as DOI: 10.1124/mol.119.116129
This article has not been copyedited and formatted. The final version may differ from this version.

Table 1. Anti-proliferative profile of ISL on various cell lines

Cell lines	Tumor types	IC_{50} (μM)
MV4-11	human acute myeloid leukemia	3.2±1.2
MOLM-13	human acute myeloid leukemia	4.9±2.1
OCI-LY10	human B cell lymphoma	20.1±6.7
A549	human lung cancer	>50
HGC-27	human gastric cancer	>50
HepG2	human hepatocellular carcinoma	>50
HCT116	human colorectal cancer	>50
MCF-10A	human mammary epithelial cell	>50
Ba/F3	Murine pro-B cell line	>50

n=3 for each experiment

Molecular Pharmacology Fast Forward. Published on August 28, 2019 as DOI: 10.1124/mol.119.116129
This article has not been copyedited and formatted. The final version may differ from this version.

Table 2. The single mutated residue of FLT3 protein with the optimized local structure.

Name	PDF Total Energy[a]	PDF Physical Energy[a]	DOPE Score[a]
4XUF.M0005	1215.77	3.72	-33513.02
4XUF.M0002	1215.78	3.75	-33512.52
4XUF.M0003	1215.78	3.71	-33512.18
4XUF.M0001	1215.78	3.76	-33512.70
4XUF.M0004	1215.95	3.74	-33511.29

[a] which was calculated by Discovery Studio (DS) 3.1 (Accelrys, Inc., USA)

Molecular Pharmacology Fast Forward. Published on August 28, 2019 as DOI: 10.1124/mol.119.116129
This article has not been copyedited and formatted. The final version may differ from this version.

Figure legend

Figure 1 ISL selectively suppressed FLT3 kinase activity and inhibited the proliferation of FLT3 dependent cells. (A) The chemical structure of ISL. (B) Kinase inhibitory activities of ISL were measured by the HTRF kit. ISL selectively inhibited FLT3 kinase activity. (C and D) The enzyme kinetic experiments were conducted with different concentrations of ATP. ISL is an ATP-competitive FLT3 inhibitor. (E) ISL selectively inhibited the proliferation of Ba/F3-FLT3-ITD cells and was non-toxic toward Ba/F3-FLT3-ITD cells rescued by IL-3. Ba/F3-FLT3-ITD cells cultured with or without IL-3 were treated with ISL for 72 h. Cell viability was measured by MTT assay. Data are representative of more than three independent experiments. (F) ISL selectively inhibited the proliferation of Ba/F3-FLT3-ITD/F691L cells and was non-toxic toward the cells rescued by IL-3. FLT3-ITD-F691L mutantion is resistant to AC220(G) and Sorafenib(H).

Figure 2 The binding mode of ISL and FLT3. (A) ISL is docked into the FLT3-wt kinase domain, demonstrating interactions between ISL and FLT3 (PDB entry 4XUF). (B) The 2-dimensional interaction map of ISL and FLT3-wt. (C) ISL is docked into the FLT3 kinase domain, showing interactions between ISL and FLT3 mutation (4XUF.M0005) in an inactive conformation. (D) The 2-dimensional interaction map of ISL and FLT3/F691L.

Molecular Pharmacology Fast Forward. Published on August 28, 2019 as DOI: 10.1124/mol.119.116129
This article has not been copyedited and formatted. The final version may differ from this version.

Figure 3 ISL induced cell cycle arrest and apoptosis in AML cells. (A and **C)** MV4-11 cells were treated with serial concentrations of ISL for 20 h. The cell cycle was measured by PI staining and flow cytometry. ISL significantly induced G0-G1 phase arrest with the decreased ratio of cells in S to G2/M phase (* $p<0.05$, ** $p<0.01$, n=3). **(B** and D**)** MV4-11 cells treated with ISL for 30 h and the apoptotic cells were defined by Annexin-V and PI co-staining. Apoptotic cells were defined as Annexin V+/PI- plus Annexin V+/PI+ cells. The ratio of apoptosis significantly increased from 3.92 ± 2.65% (control) to 53.11 ± 11.31% (ISL 40 μM) (* $p<0.05$, ** $p<0.01$, *** $p<0.001$, n=3). Sunitinib, as positive control, also significantly induced cell cycle arrest and apoptosis in AML cells.

Figure 4 ISL inhibited the activation of FLT3 signal and regulated the expressions of apoptosis-related protein. (A) After a 16-hours of treatment with ISL, the phosphorylation of FLT3 and downstream signal proteins was assessed using Western blot analysis. Sunitinib was considered as positive control. (B) The cells lysate of MV4-11 cells treated with ISL for 30 hours was also analyzed using anti-caspase-3 antibody, and the results indicated a significant dose-dependent decrease in pro–caspase-3 levels and a dose-dependent increase in cleaved caspase-3 levels with increasing concentrations of ISL. (a) The relative densitometric value of the western blot band were analyzed using image analyzing software. Statistical analysis was performed to consider the differences (*, $P<0.05$; **, $P<0.01$, n=3).

Molecular Pharmacology Fast Forward. Published on August 28, 2019 as DOI: 10.1124/mol.119.116129
This article has not been copyedited and formatted. The final version may differ from this version.

Figure 5 *In vivo* effects of ISL against s.c. and BM MV4-11 tumor models. (A) MV4-11 cells (6×10^6/mouse) were s.c. injected into NOD-SCID mice, and oral treatment with ISL was initiated when the tumors grew to 100~200 mm^3. ISL significantly inhibited the MV4-11 tumor growth at the doses of 100 ($p<0.01$, n=6), 50 ($p<0.01$, n=6) or 25 ($p<0.05$, n=6) mg/kg/d p.o.; meanwhile, sunitinib as positive control exhibited marked anti-tumor activity ($p<0.01$, n=6). **(B)** The mice body weights among the groups were analyzed after 18 days of treatment. The mean ± SD were also presented (n=6). **(C)** Kaplan-Meier plot for survival analysis. MV4-11 cells (5×10^6/mouse) were intravenously injected into NOD-SCID mice, and treated with an oral dose of ISL after 20 days of inoculation. Survival was determined by observation when the animals demonstrated hind-limb paralysis or became moribund. Finally, ISL significantly prolonged the survival time of bone marrow engraftment AML mice at the doses of 100 ($p<0.001$, n=10), 50 ($p<0.01$, n=10) mg/kg/d p.o.. **(D)** After 18-day of ISL treatment, MV4-11 tumors were harvested, fixed and subjected to immunohistochemistry using Ki-67, p-Erk1/2 antibodies, followed by TUNEL assay. The findings of the study showed that ISL significantly inhibited the expression of Ki67, the activation of Erk1/2, and induced apoptosis *in vivo*. **(E and e)** MV4-11 tumors were also lysated for western blot analysis. The in vivo expression of Ki67 and activation of Erk1/2 was corroborated by western blots assay. The relative densitometric value (to the average value of control group) of the western blot band were analyzed using image analyzing software. Statistical analysis was performed to consider the differences ($P<0.05$; **, $P<0.01$, n=3). **(F)** After 30 days of

Molecular Pharmacology Fast Forward. Published on August 28, 2019 as DOI: 10.1124/mol.119.116129
This article has not been copyedited and formatted. The final version may differ from this version.

inoculation, bone marrow engraftment mice were treated with vehicle or ISL (100 mg/kg/d) for 10 days. Subsequently, paraffin sections of bone marrow from the vehicle or ISL-treated mice were stained with Ki67. The representative result is shown. **(G)** The analysis demonstrated that ISL had no influence on the micro-morphology of normal tissues including heart, liver, spleen, lung, and kidney.

Molecular Pharmacology Fast Forward. Published on August 28, 2019 as DOI: 10.1124/mol.119.116129
This article has not been copyedited and formatted. The final version may differ from this version.

Figure 1

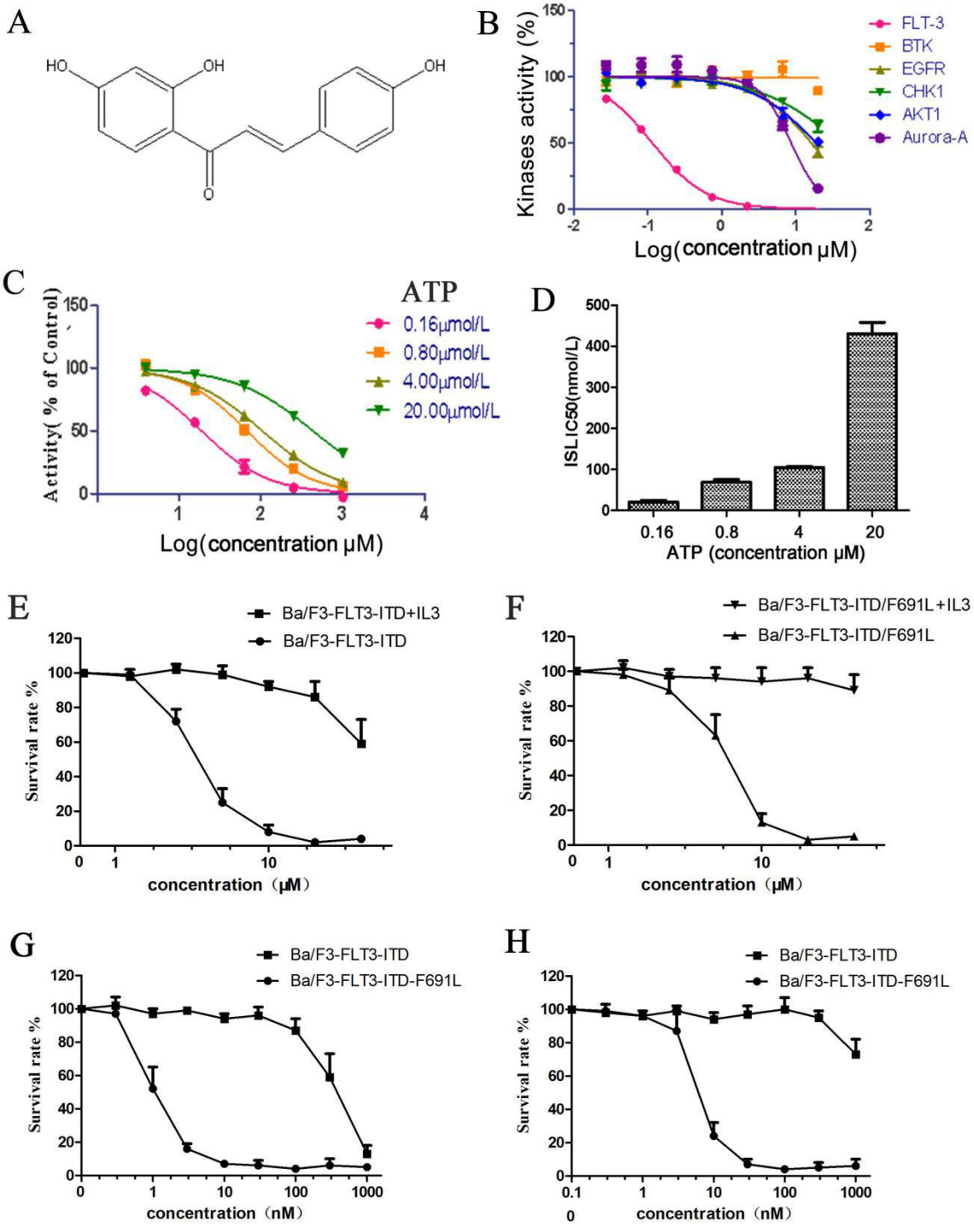

Molecular Pharmacology Fast Forward. Published on August 28, 2019 as DOI: 10.1124/mol.119.116129
This article has not been copyedited and formatted. The final version may differ from this version.

Figure 2

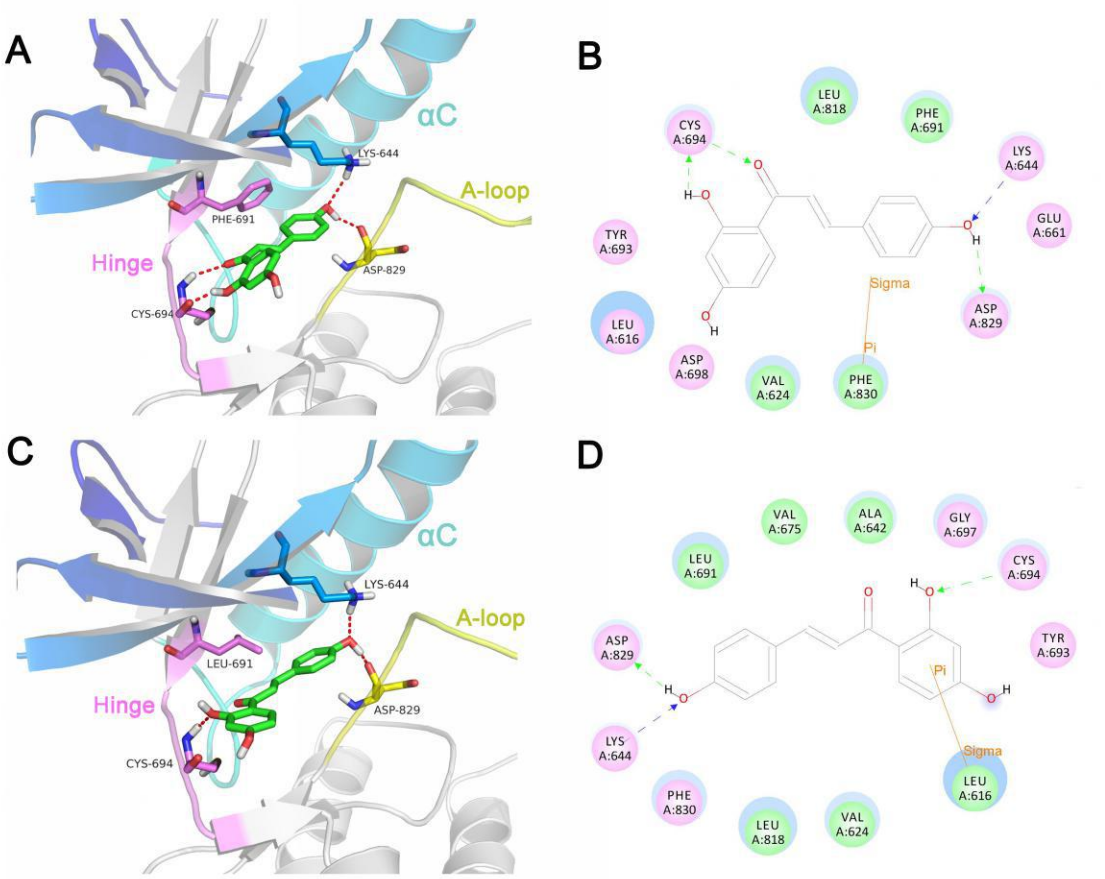

Molecular Pharmacology Fast Forward. Published on August 28, 2019 as DOI: 10.1124/mol.119.116129
This article has not been copyedited and formatted. The final version may differ from this version.

Figure 3

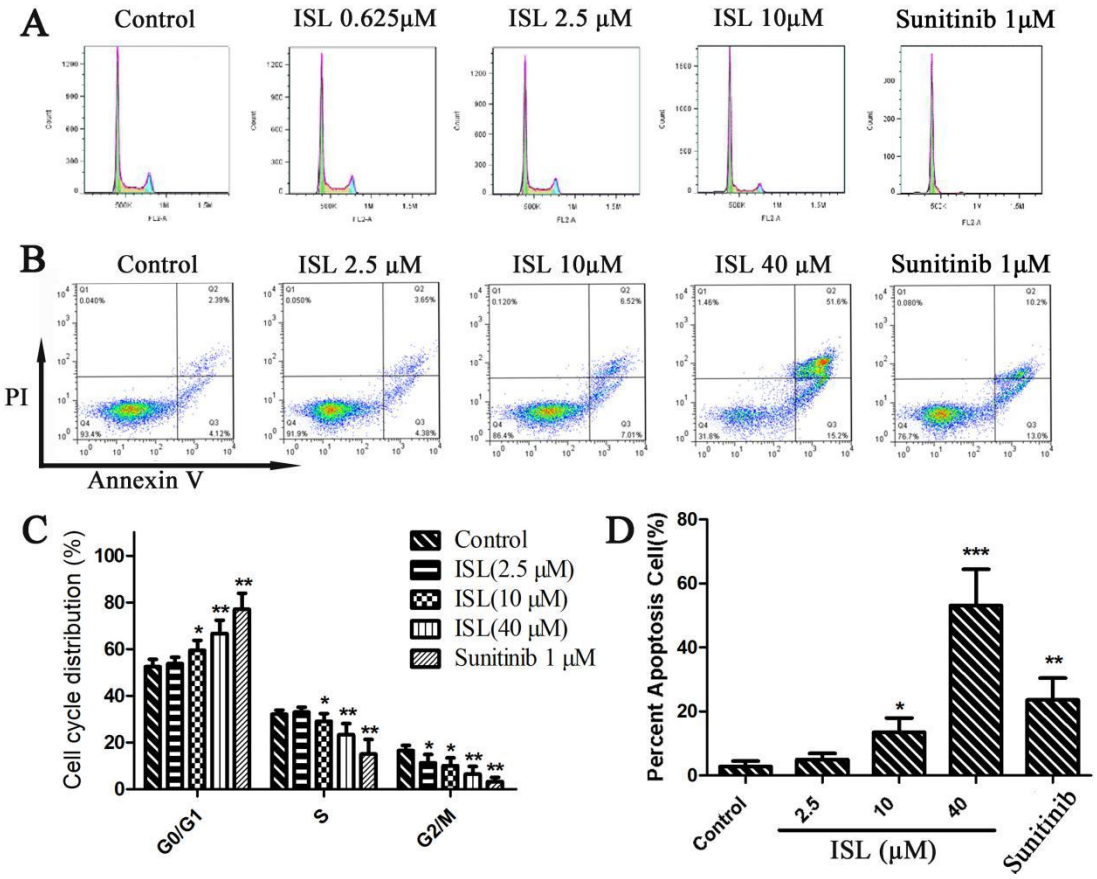

Molecular Pharmacology Fast Forward. Published on August 28, 2019 as DOI: 10.1124/mol.119.116129
This article has not been copyedited and formatted. The final version may differ from this version.

Figure 4

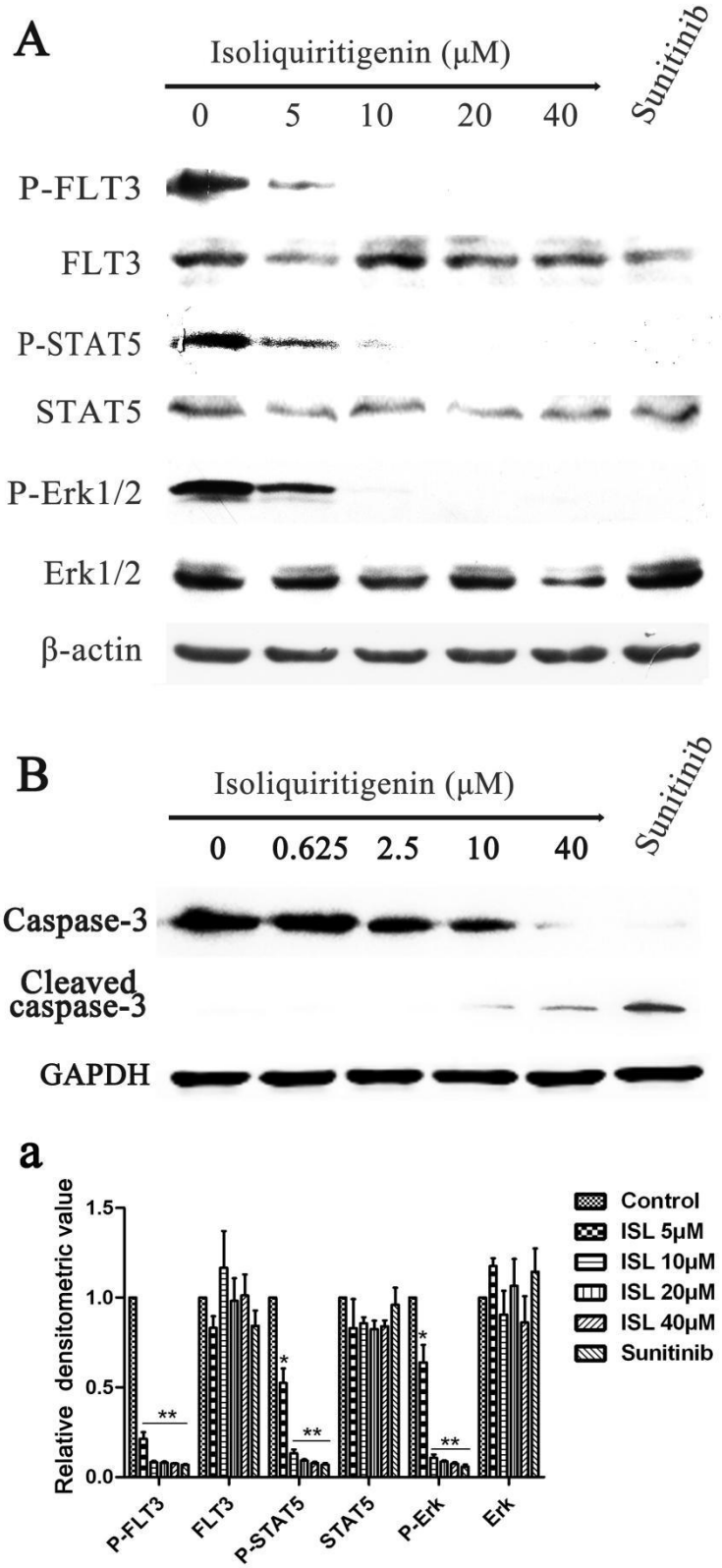

Molecular Pharmacology Fast Forward. Published on August 28, 2019 as DOI: 10.1124/mol.119.116129
This article has not been copyedited and formatted. The final version may differ from this version.

Figure 5